Journal of Computational and Applied Mathematics 236 (2011) 867–877

Contents lists available at SciVerse ScienceDirect

Journal of Computational and Applied Mathematics

journal homepage: www.elsevier.com/locate/cam

A finite-element mechanical contact model based on Mindlin–Reissner shell theory for a three-dimensional human body and garment☆

Ruomei Wang [a,*], Yu Liu [a,*], Xiaonan Luo [a], Yi Li [b], Shuai Ji [a]

[a] School of Information Science and Technology, Sun Yat-Sen University, Guangzhou 510275, China

[b] Institute of Textile and Clothing, Hong Kong Polytechnic University, Hunghom, Kowloon, Hong Kong

ARTICLE INFO

Keywords:
Garment simulation
Finite element
Shear lock
Contact model

ABSTRACT

Efficient numerical methods for describing a garment's mechanical behavior during wear have been identified as the key technology for garment simulation. This paper presents a finite-element mechanical contact model based on Mindlin–Reissner shell theory for a three-dimensional human body and garment. In this model, the human body and the garment are meshed as basic contact cells, these contact cells between the human body and the garment are defined as the contact pair to describe the contact relationship, and the mathematical formulation of the finite-element model is defined to describe the strain–stress performance of the three-dimensional human body and garment system. By using the solution given by the computer code and the programs specifically developed, the calculations of the mechanics in the basic cells of the human body and the garment have been able to be carried out. The simulation results show that the model of rationality, a good simulation results and simulation efficiency.

1. Introduction

The finite-element approach employing a shell element has been used by a number of researchers. It has a rigorous mechanical basis and can be applied in different areas. Finite elements have been applied to yarn mechanics and fibrous assemblies for decades, but a completely rigorous mechanical analysis approach using a finite-element model for a human body and a garment has never been completed. In this paper, a finite-element mechanical contact model based on Mindlin–Reissner shell theory for a three-dimensional (3D) human body and garment is reported.

A garment is a typical object with small bending rigidity compared with its in-plane rigidity, and as such has been studied by a number of researchers. Typical numerical methods have been proposed to simulate the large displacement and small strain problem of the draped cloth within the framework of continuum mechanics. The garment's mechanical simulation process needs to construct 3D garment geometric data and a mechanical analysis model. In order to construct the meshed 3D garment data model, Wang reported a geometrical method to generate the 3D garment data to be used in the mechanical analysis [1,2]. Gao reported a subdivision method to construct the 3D virtual garment [3]. Dai reported a finite-element model to simulate compression stockings using ABAQUS [4]. Zhang presented a numerical simulation method using the finite-element method for garment pressure [5]. Terzopoulos et al. introduced a deformable model based on the variational principle; the model was discretized by a finite-difference method [6]. Collier et al. studied the draping behavior of fabrics by using a geometric nonlinear finite-element method based on classical plate theory [7]. However, only the

☆ This work is supported by the NSFC Guangdong Joint Fund (61073131, U0735001, U0935004), the National Key Technology R&D Program of China (No. 2007BAH13B01), and the 973 Program of China (No. 2006CB303106).

* Corresponding author.
E-mail addresses: isswrm@mail.sysu.edu.cn (R. Wang), 6zly@21cn.com (Y. Liu).

0377-0427/$ – see front matter © 2011 Elsevier B.V. All rights reserved.
doi:10.1016/j.cam.2011.05.017

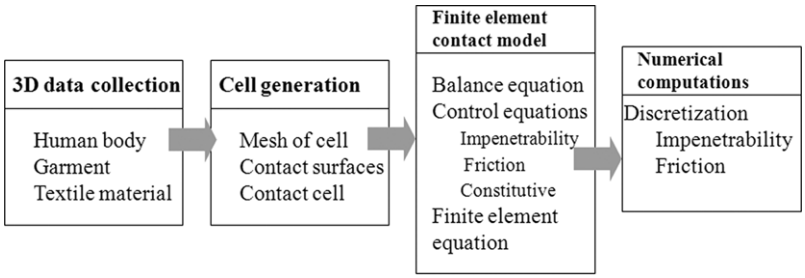

Fig. 1. Architecture of the contact model.

geometrically nonlinear terms of the transverse displacement were included in their definition of the strains. Zhao et al. proposed a geometric–physical model by combining thin-plate bending theory with the geometric constraints of fabric inextensibility [8]. Kang et al. simulated the draping of woven fabric based on plate theory using the Mindlin–Reissner hypothesis [9], Geometrical nonlinearity and orthotropy of the fabric were considered in their finite-element analysis. Gan et al. developed a model using shell/plate elements, fabric deformation characterized by large displacements and rotations but small strains, analyzed by using a geometric nonlinear finite-element method [10]. In recent years, some 3D clothing computer-aided design (CAD) technologies have been reported too. Meng [11] reported an interactive virtual try-on clothing design system, and Wang [12] introduced an interactive 3D garment design with constrained contour curves and style curves.

However, the influences caused by the garment structure and the frictions between the human body and garment and the transverse shear in garment are not taken into account in the studies mentioned above. This paper presents a finite-element mechanical contact model based on Mindlin–Reissner shell theory for a 3D human body and garment, which can be used to treat the garment as a flexible shell based on elasticity theory with the corresponding 3D human body–garment contact model formulated. It can simulate the mechanical behavior of the human body and garment during wear. In this model, the human body and garment are meshed as basic cells, contact cells between the human body and the garment are defined to describe the contact relationship, and the mathematical formulation of the finite-element model is defined to describe the strain–stress performance of the 3D human body and garment system. By using the solution given by the computer code and the programs specifically developed, the calculations of the mechanics in the basic cells of the human body and the garment have been able to be carried out. Results of the mechanical behavior of human body and garment during wear have obtained.

2. Finite-element mathematical formulations

Efficient numerical methods for describing a garment's mechanical behavior during wear have been identified as the key to the development of successful CAD systems for garment simulation. The finite-element method is used to solve this problem because of its flexible shell based on elasticity theory.

The finite-element mechanical contact model based on Mindlin–Reissner shell theory for a 3D human body and garment includes some mathematical formulations. Fig. 1 shows the model architecture.

2.1. Contact model assumptions and descriptions

The relationship between a human body and a garment during wear is complex. In this system, considering the requirement of computation and simulation, the model is based on following assumptions.

(a) The human body is a shell with very limited flexibility.
(b) The garment is an elastic, continuous shell with material linearity and geometric nonlinearity.
(c) The contact between the body and the garment is dynamic because of the contact feature that the magnitude of the contact interface is comparable to the effective surfaces of the body and the garment [13].

To use finite-element methods (FEMs), the contact forces must be applied to each nodal point of the finite-element mesh. Based on the assumptions above, the mesh cell of the 3D human body and garment is described by a four-node thin-plate shell element. Fig. 2 shows the four-node thin-plate shell element.

A four-node thin-plate shell element has the performances about bending and dissepimental, it can be loaded in plate. Every element can be translated and rotated in the x, y, and z axes. This gives a good way to use this element to simulate a 3D garment and human body. At the same time, using these types of element can decrease the model complexity and increase the simulation efficiency.

According to the four-node thin-plate shell element, the 3D human body and garment can be described as a set of shell elements; these shell elements are constructed as contact cells, and therefore the contact analysis model between the human body and the garment can be constructed.

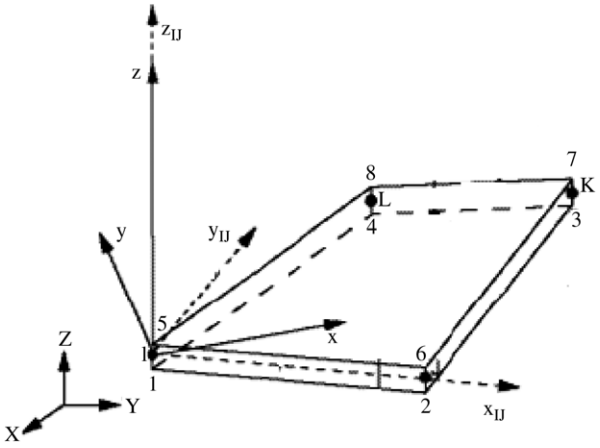

Fig. 2. Four-node thin-plate shell element.

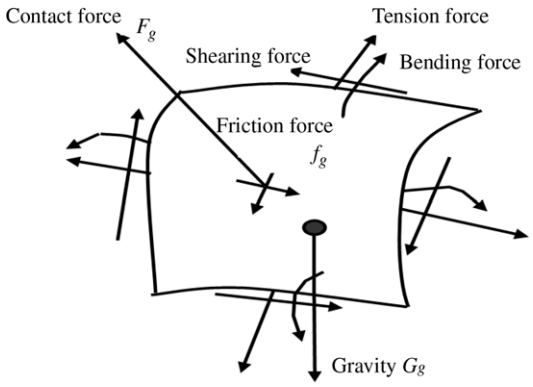

Fig. 3. The external forces and internal stresses on the garment.

By the virtual displacement principle and continuum hypothesis [14], the contact balance equation between the human body and the garment can be written as

$$\int_v \tau_{ij}\delta e_{ij}\mathrm{d}V - W_L - W_I - W_C = \int_{v^G} \tau_{ij}^G \delta e_{ij}^G \mathrm{d}V - W_L^G - W_I^G - W_C^G = 0, \tag{1}$$

where W_L is the virtual work by the external force, W_C is the virtual work by the contact force, W_I is the virtual work by the inertia force, and u_i is the displacement.

Here,

$$W_L = \int_{S_\sigma} f_g \delta u_i \mathrm{d}S + \int_{V^G} \rho_g g_i \delta u_i \mathrm{d}V \tag{2}$$

$$W_I = \int_{V^G} -\rho_g \ddot{u}_i \delta u_i \mathrm{d}V \approx 0 \tag{3}$$

$$W_c = \int_{S_c^G} F_g^\delta u_i \mathrm{d}S, \tag{4}$$

where ρ_g is the mass density, f_g is the friction, g is the acceleration due to gravity, and F_g is the contact force on garment. Fig. 3 shows these definitions.

In the mathematical model, there are other restrictive conditions.

(a) The deformation in the direction of the shell thickness is ignored, and the normal on the surface during deformation is still kept as the surface's normal.
(b) Transverse bending of the shell and displacement in surface are out of the picture.

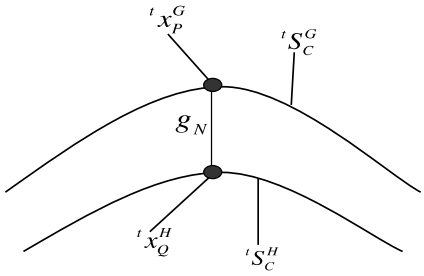

Fig. 4. The two boundary points in the human body and garment.

2.2. Control equations

In order to compute the contact model of the human body and garment, some control equations are important.

2.2.1. Impenetrability conditions

In the simulation, in order to protect infiltration between the garment and the human body, the contact cell positions V^G and V^H of the garment ${}^tS_C^G$ and the human body ${}^tS_C^H$ are not allowed to run through each other during the contact process. So the impenetrability conditions are important. Fig. 4 shows the two boundary points in the human body and garment. P is any point in the garment, and ${}^tg$ is the distance between P and Q at time t.

$$ {}^tg = g({}^tx_P^G, t) = \left|{}^tx_P^G - {}^tx_Q^H\right| = \min\left|{}^tx_P^G - {}^tx^H\right|, \tag{5} $$

where ${}^tg_N$ is the distance between P and Q in the normal direction at time t.

$$ {}^tg_N = g({}^tx_P^G, t) = ({}^tx_P^G - {}^tx_Q^H)\,{}^tn_Q^H, \tag{6} $$

where ${}^tx_P^G$ is the coordinate of point P at step t in ${}^tS^G$. So we can present the impenetrability condition, given in Eq. (7).

$$ {}^tg_N = g({}^tx_P^G, t) = ({}^tx_P^G - {}^tx_Q^H)\,{}^tn_Q^H \geq 0. \tag{7} $$

2.2.2. Friction restriction

Similarly, according to the Coulomb friction model, there is a friction restrictive equation.

$$ \left|{}^tF_T^G\right| = \left[\left({}^tF_1^G\right)^2 + \left({}^tF_2^G\right)^2\right]^{1/2} \leq \mu\left|{}^tF_N^G\right|. \tag{8} $$

Here, μ is the friction coefficient, ${}^tF_T^G$ is the contact force in the cutting direction, and ${}^tF_N^G$ is the contact force in the normal direction. When $\left|{}^tF_T^G\right| < \mu\left|{}^tF_N^G\right|$, there is no relative motion between the contact surfaces in the cutting direction, and when $\left|{}^tF_T^G\right| = \mu\left|{}^tF_N^G\right|$, there is relative motion between the contact surfaces in the cutting direction.

2.2.3. Constitutive equations of garment material

The constitutive equations are material dependent. For linearly elastic materials, the stress–strain relation may be given by the generalized Hooke's law [15], i.e.,

$$ {}^ts_{ij} = c_{ijkl}\,{}^t\varepsilon_{kl}, \tag{9} $$

where c_{ijkl} are material constants, s_{ij} is a component of the second Piola–Kirchhoff stress tensor that is related to the Cauchy stress component $\sigma_{ij}(x)$, and ε_{kl} is a component of the Green–Lagrange strain tensor to describe the deformation of geometric nonlinearity, which consists of linear and nonlinear components:

$$ {}^te_{ij} = \left({}^tu_{i,j} + {}^tu_{j,i}\right)/2, \qquad {}^t\eta_{ij} = {}^tu_{k,i}\,{}^tu_{k,j}/2, \tag{10} $$

where ${}^tu_{i,j} = \frac{\partial {}^tu_i}{\partial {}^tx_j}$.

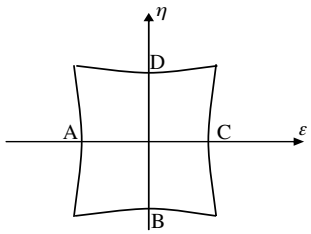

Fig. 5. Mid-surfaces of the four-node shell.

2.3. Finite-element equations in the contact system

Choosing the deformed configuration as the reference configuration, the position vector of a point Φ in the shell in the current configuration is defined as

$$\Phi(\varepsilon, \eta, \zeta) = \phi(\varepsilon, \eta) + \zeta n(\varepsilon, \eta) \quad (-h/2 \le \zeta \le h/2), \tag{11}$$

where ϕ is a position vector locating points on the shell's mid-surface (reference surface). The coordinate ζ measures the distance between the mid-surface and points off the mid-surface along n. h is the shell thickness. ε and η are curvilinear coordinates. The vector n is a unit vector normal to the shell mid-surface in the reference configuration.

The evolution of the director vectors n during motion of the shell depends on an orthogonal transformation matrix Λ [16]. Let $n = \Lambda E$, where Λ is an orthogonal matrix such that $\Lambda\Lambda^T = I$ and E is an initially fixed unit vector. At any point on the shell, this matrix is related to the unit director according to $\Lambda = (E \cdot n) I + E \times n + \frac{1}{1+E\cdot n}(E \times n) \otimes (E \times n)$, where $\otimes$ represents a tensor outer product operator.

In the four-node shell element, the kinematics variables consist of the displacement vector u and the director vector n. Within a single element, the kinematics variables are approximated by interpolation.

$$u(\varepsilon, \eta) = \sum_{1}^{4} N^I(\varepsilon, \eta) u_I,$$

$$n(\varepsilon, \eta) = \sum_{1}^{4} N^I(\varepsilon, \eta) n_I,$$

where $N^I(\varepsilon, \eta)$ are the standard bilinear shape functions $N^I = 1/4\left(1 + \varepsilon\varepsilon^I\right)\left(1 + \eta\eta^I\right)$ and u_I and n_I are the displacement vector and the director of nodes, respectively.

Shear locking is commonly observed in the analysis of a thin plate or shell [14]. To avoid this phenomenon, the interpolation method of the shear strain based on the assumed strain field is adopted [17]. This method prescribes the shear to vary linearly between two opposite element edges.

$$\gamma_\varepsilon = \frac{1}{2}\left[(1-\eta)\gamma_\varepsilon^B + (1+\eta)\gamma_\varepsilon^D\right]$$

$$\gamma_\eta = \frac{1}{2}\left[(1-\varepsilon)\gamma_\eta^A + (1+\varepsilon)\gamma_\eta^C\right]$$

where A, B, C, and D denote the middle points of the element edges, as shown in Fig. 5.

According to Eq. (11), the finite-element contact model in a 3D human body and garment can be described by the following matrix equation:

$$K(\phi, n) u = F_{\text{ext}} - P(\phi, n). \tag{12}$$

Here, $K(\phi, n)$ is the rigidity matrix:

$$K(\phi, n) = \int_V B^T D B \mathrm{d}V. \tag{13}$$

B is the strain matrix, $P(\phi, n)$ is the internal force, F_{ext} is the external force, u is a function of the mid-surface displacement vector $\Delta\phi$, matrix variation $\Delta\Lambda$, $\Delta\phi$ is used to update the point position in the mid-surface, and $\Delta\Lambda$ is used to update the normal vector in the mid-surface.

3. Numerical computations in contact model

3.1. Discretization of impenetrability conditions

At time $t + \Delta t$, Eq. (7) can be written as

$$ {}^{t+\Delta t}g_N = g({}^{t+\Delta t}x_P^G, t) = ({}^{t+\Delta t}x_P^G - {}^{t+\Delta t}x_Q^H)^{t+\Delta t}n_Q^H \geq 0. \tag{14} $$

The garment position function ${}^{t+\Delta t}x^G$ and human body position function ${}^{t+\Delta t}x^H$ can be written as

$$ {}^{t+\Delta t}x^G = {}^{t}x^G + \Delta u^G $$
$$ {}^{t+\Delta t}x^H = {}^{t}x^H + \Delta u^H, $$

where Δu^G and Δu^H are displacement increments from time t to time $t + \Delta t$.

$$ \Delta u^G = {}^{t+\Delta t}u^G - {}^{t}u^G $$
$$ \Delta u^H = {}^{t+\Delta t}u^H - {}^{t}u^H. $$

From the equations above, the impenetrability conditions can be given as follows:

$$ \begin{aligned} {}^{t+\Delta t}g_N &= ({}^{t+\Delta t}x^G - {}^{t+\Delta t}x^H)^{t+\Delta t}n^H \\ &= (\Delta u^G - \Delta u^H)^{t+\Delta t}n^H + ({}^{t}x^G - {}^{t}x^H)^{t+\Delta t}n^H \\ &= u_N^G - u_N^H + {}^{t}\overline{g}_N \geq 0 \end{aligned} \tag{15} $$

$$ u_N^G = \Delta u^G \cdot {}^{t+\Delta t}n^H $$
$$ u_N^H = \Delta u^H \cdot {}^{t+\Delta t}n^H $$
$$ {}^{t}\overline{g}_N = ({}^{t}x^G - {}^{t}x^H)^{t+\Delta t}n^H. $$

3.2. Discretization of friction conditions

The condition without relative slip in binder contact can be written as follows:

$$ \Delta\overline{u}_T = \Delta u_T^G - \Delta u_T^H = 0 \quad \text{when } \left|{}^{t}F_T^G\right| < \mu \left|{}^{t}F_N^H\right|. \tag{16} $$

Here, Δu_T^G and Δu_T^H are tangential components of Δu^A and Δu^B, i.e., the tangential displacement increments of the contact node from time t to time $t + \Delta t$. $\Delta\overline{u}_T$ relativity tangential components of contact node.

The condition with relative slip in slither contact can be written as follows:

$$ \Delta\overline{u}_T = \Delta u_T^G - \Delta u_T^H \neq 0 \quad \text{when } \left|{}^{t}F_T^G\right| = \mu \left|{}^{t}F_N^G\right|. $$

4. Modeling simulation and analysis

The contact analysis algorithm has two components.

(a) The definition of contact areas of the human body and garment.
(b) Computation of the contact model.

4.1. Simulation algorithm

The main algorithm for computational simulation of the finite-element contact model is as follows.

```
(1) Define the three-dimensional parameters of the garment and human body
(2) Define the material data used in the garment
(3) Mesh process and contact cell construction between human body and garment
(4)   For each time step
(5)     For every contact cell of the garment
(6)       Calculate all impenetrability condition equations discretized at contact cells
(7)       Calculate all friction condition equations discretized at contact cells
(8)     Solve all position vectors of a point
(9)       Calculate all normal vectors of a point
(10)        Update every contact cell position vector for
(11) Store the strain–stress value during the simulation process to the data file
(12) Simulation results visualization and analysis
```

Table 1
Material parameters of the human body.

Density (g/cm^3)	Tensile modulus (gf/cm^2)	Poisson's ratio
0.6	205	0.3

Table 2
Material parameters of fabrics.

Fabric	Density (g/cm^3)	Shear modulus (gf/cm^2)	Tensile modulus (gf/cm^2)		Thickness (cm)	Bend modulus (gf/cm^2)	
			Warp	Weft		Warp	Weft
Nylon	0.408	2546.1	11 867.7	13 409.7	0.062	3.725	4.576
Cotton	0.404	1105.8	11 712.5	11 070.9	0.046	1.494	1.26

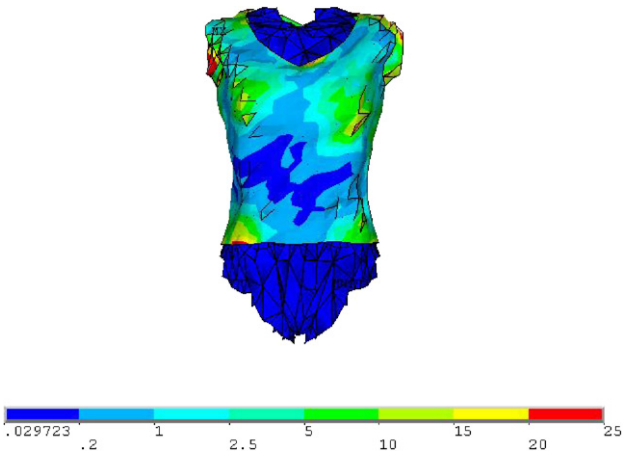

Fig. 6. Pressure distribution of cotton gilet front.

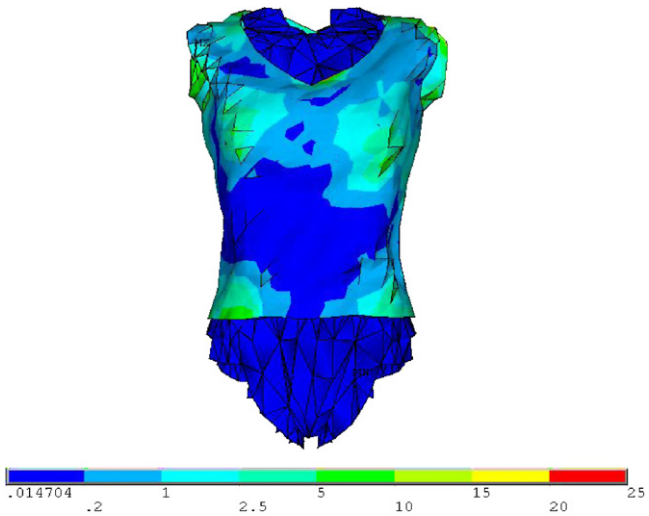

Fig. 7. Pressure distribution of nylon gilet, front.

4.2. Results and discussion

A finite-element analysis process has been implemented based on the method described above. The case studies aim to illustrate the effectiveness of the model for describing the pressure distributions in a human body and in garments which have different material properties or structure.

The material values of the human body are summarized in Table 1 [18].

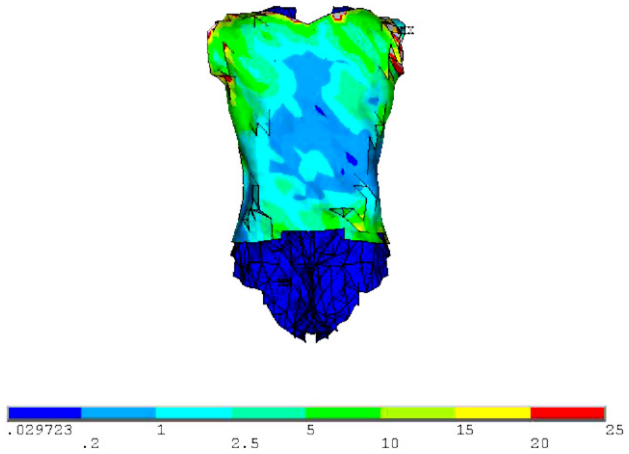

Fig. 8. Pressure distribution of cotton gilet, back.

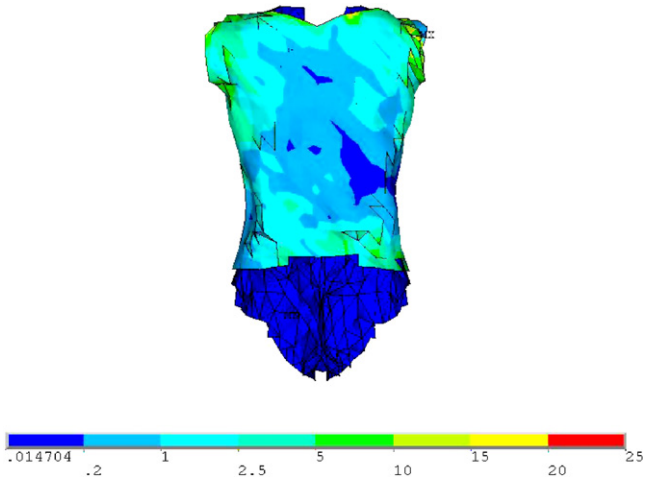

Fig. 9. Pressure distribution of nylon gilet, back.

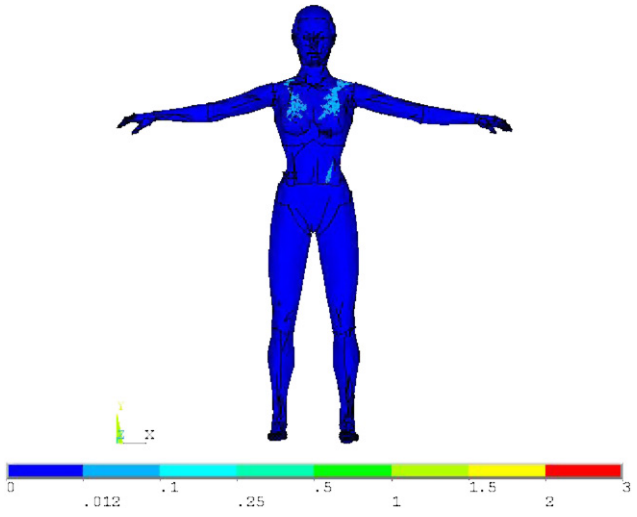

Fig. 10. Pressure distribution of the body wearing the cotton gilet, front.

Two sets of garments, which are made from a cotton gilet and a nylon gilet with the same style and size, and a cotton one-piece dress are used in the numerical simulation.

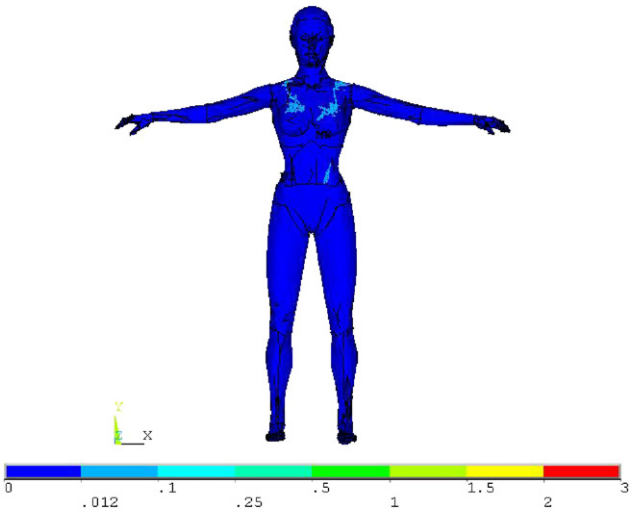

Fig. 11. Pressure distribution of the body wearing the nylon gilet, front.

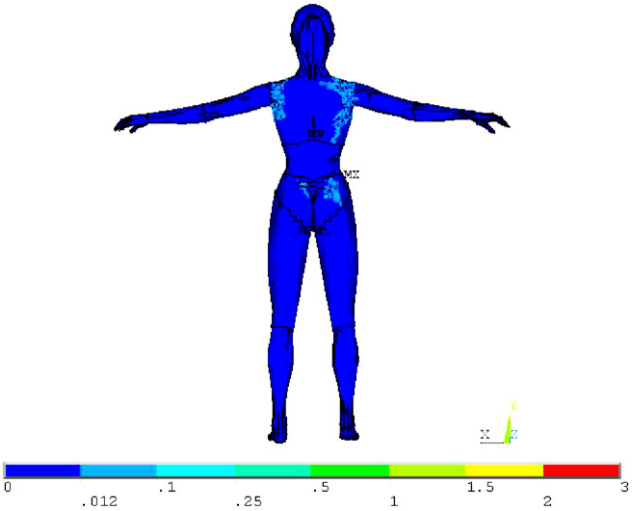

Fig. 12. Pressure distribution of the body wearing the cotton gilet, back.

The material parameters were measured by using the Kawabata Evaluation System. The measured values are summarized in Table 2 [19].

Figs. 6–15 show the simulation results during wear for garments with different material and different style.

Figs. 6 and 8 show the pressure distributions viewed from the front and back of the cotton gilet. Similarly, Figs. 7 and 9 show the pressure distributions viewed from the front and back of the nylon gilet. From the pressure contour plot, one can see that the pressure is distributed unevenly over different parts of the body. Most of the areas covered by the clothing have relatively low pressures, and high-pressure zones occur in the areas of the waist and upper chest with pressures.

Figs. 10 and 12 show the pressure distributions in the body wearing the cotton gilet. Similarly, Figs. 11 and 13 show the pressure distributions in the body wearing the nylon gilet, which tend to be similar to those when wearing the cotton gilet. However, the low-pressure zones are much greater and the high-pressure zones are much smaller. High-pressure zones are observed in the waist and upper chest with pressure. Comparing the pressure contour plots, it is evident that the pressure induced on the body by the denim garments is significantly higher than that by the knitted garments, suggesting that fiber and fabric mechanical properties affect the garment pressure distribution and comfort perception.

Figs. 14 and 15 show the pressure distributions viewed from the front and back of the cotton one-piece dress. Most of the areas covered by the clothing have relatively low pressures, but high-pressure zones occur in the areas of the waist and upper chest. The contact is in the shoulder, chest, back, and buttocks. The difference in contact area between the cotton gilet and the cotton one-piece dress is due to the garment structures.

These results indicate that the model is effective in describing the pressure distributions for both a human body and garments that are made of materials with different physical properties or that have different structures.

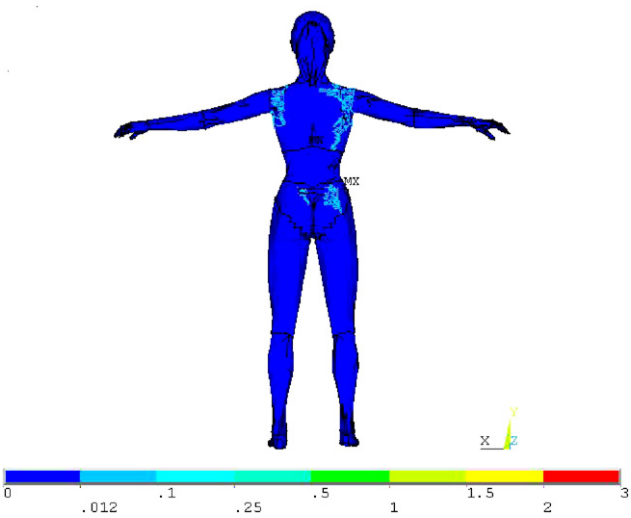

Fig. 13. Pressure distribution of the body wearing the nylon gilet, back.

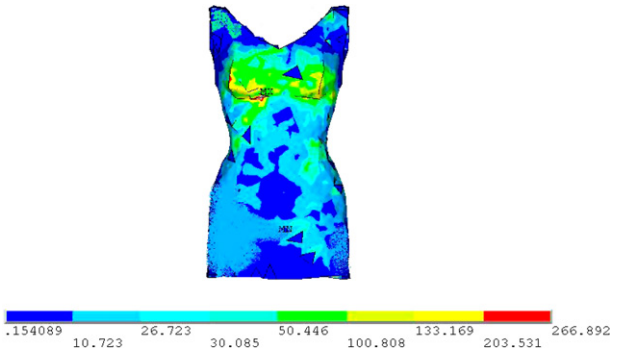

Fig. 14. Pressure distribution of the body wearing the cotton one-piece dress, front.

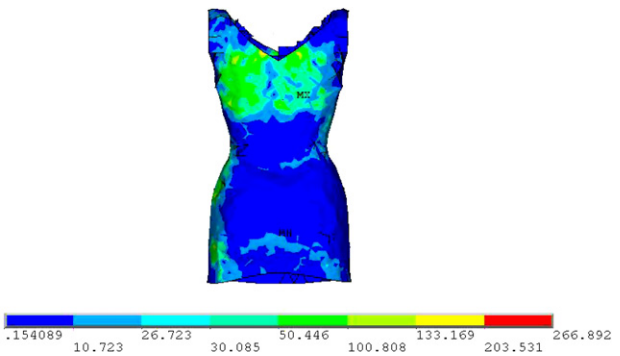

Fig. 15. Pressure distribution of the body wearing the cotton one-piece dress, back.

5. Conclusions

This paper presents a finite-element mechanical contact model based on Mindlin–Reissner shell theory for a 3D human body and garment. In this model, the human body and garment are meshed as basic cells, contact cells between human body and garment are defined to describe the contact relationship, and the mathematical formulation of the finite-element model is defined to describe the strain–stress performance of the 3D human body and garment system. According to the simulation, the results can be summarized as follows. (1) Different garment materials will affect the simulation result, i.e., the finite-element contact model based on Mindlin–Reissner shell theory has good expressive properties for different materials. (2) The model can simulate the contact strain and displacement between a human body and a garment during wear. (3) Four-nodes thin-plate shell elements have a simple structure, which is good for solving the physical equation, and the model has good simulation efficiency.

Acknowledgments

The authors would like to thank the National Science Fund for Distinguished Young Scholars and the Key Program of NSFC-Guangdong Joint Funds and Hong Kong Innovation Technology Commission for funding this research through the project (61073131, No. U0935004, No. U0735001, ITP/030/08TP).

References

[1] X.L. Ruomei Wang, Yi Li, Representation and Conversion of Bezier surfaces in multivariate *B*-form, Journal of Computational and Applied Mathematics 195 (1–2) (2006) 206–211.
[2] Y.L. Ruomei Wang, Xiaonan Luo, Xin Zhang, Visualization Application in Clothing Biomechanical Design, in: Lecture Notes, 2006, pp. 522–529.
[3] C. Gao, Computer Simulation and Modeling Techniques for 3D Virtual Garment, in: Computer Science, Zhongshan University, Guangzhou, 2004.
[4] Y. Li, X.-Q. Dai, Biomechanical Engineering of Textiles and Clothing, Woodhead Publishing Limited, Cambridge, England, 2006.
[5] X. Zhang, K.W. Yeung, Y. Li, Numerical simulation of 3D dynamic garment pressure, Textile Research Journal 72 (3) (2002) 245–252.
[6] D. Terzopoulos, et al. Elastically deformable models, in: SIGGRAPH, 1987.
[7] J.R. Collier, et al., Drape prediction by means of finite-element analysis, Journal of the Textile Institute 82 (1) (1991) 96–107.
[8] Zhao YF, Tan ST, A model for simulating flexible surfaces of cloth objects, Computer & Structure (1997) 133–147. W.T.
[9] T.J. Kang, W.R. Yu, K. Chung, Drape simulation of woven fabric using the finite-element method, Journal of the Textile Institute 86 (4) (1995) 635–648.
[10] L. Gan, N.G. Ly, A study of fabric deformation using nonlinear finite elements, Textile Research Journal 65 (11) (1995) 660–668.
[11] Yuwei Meng, P.Y. Mok, X. Jin, Interactive virtual try-on clothing design systems, Computer-Aided Design 42 (4) (2010) 310–321.
[12] Jin Wang, G. Lu, Weilong Li, Long Chen, Yoshiyuki Sakaguti, Interactive 3D garment design with constrained contour curves and style curves, Computer-Aided Design 4 (9) (2009) 614–625.
[13] K.L. Hatch, Textile Science, West Publishing Company, USA, 1993, New York.
[14] M.C. Wang, Finite Element Method, Tsinghua University Press, Beijing, 2003.
[15] J Pratt, G. West, Pressure Garments: A Manual on their Design and Fabrication, Bath Press, UK, 1995.
[16] J.W. Eischen, S. Deng, T.G. Clapp, Finite-element modeling and control of flexible fabric parts, IEEE Computer Graphics and Applications 16 (5) (1996) 71–80.
[17] EN Dvorkin, K. Bathe, A continuum mechanics based four node shell element for general nonlinear analysis, Engineering with Computers (1984) 77–88.
[18] W. X, Simulation of Car Crash with Dummy Inside, ChongQing University, ChongQing, 2003.
[19] Z. QF, The finite element method of fabric forming simulation. Northwestern Polytechnical University: Xi'an, 2002.